Research Article **Open Access**

Ján Viňáš*, Ľuboš Kaščák, and Miroslav Greš

Optimization of resistance spot welding parameters for microalloyed steel sheets

DOI 10.1515/eng-2016-0069
Received Jul 25, 2016; accepted Oct 10, 2016

Abstract: The paper presents the results of resistance spot welding of hot-dip galvanized microalloyed steel sheets used in car body production. The spot welds were made with various welding currents and welding time values, but with a constant pressing force of welding electrodes. The welding current and welding time are the dominant characteristics in spot welding that affect the quality of spot welds, as well as their dimensions and load-bearing capacity. The load-bearing capacity of welded joints was evaluated by tensile test according to STN 05 1122 standard and dimensions and inner defects were evaluated by metallographic analysis by light optical microscope. The welding parameters of investigated microalloyed steel sheets were optimized for resistance spot welding on the pneumatic welding machine BPK 20.

Keywords: resistance spot welding; microalloyed steels; load-bearing capacity; metallography

1 Introduction

Resistance spot welding (RSW) plays an important role in the automotive industry because of its high efficiency, suitability and relatively low cost [1]. This joining method is also used in the aerospace industry, medical devices and electronics. The weld is made using a combination of welding parameters, such as welding current, welding time as well as electrode pressure between two water-cooled copper-based electrodes. Welding current is supplied to the sheets via the two welding electrodes. High joule heating is created at the faying surface. The joint is completed by solidification of the spot weld caused by cooling through the welding electrodes. The electrodes' force is applied to clamp the workpiece, then electric current is switched on to pass through the workpiece, followed by post-weld cooling of the weld nugget [2–4].

A wide variety of metal sheets up to thickness of 3 mm can be joined by the RSW method [5]. The present requirements for car weight reduction, have brought new types of steels to automotive industry. Advanced high strength steels (AHSS) have been introduced into vehicle designs in an effort to increase the collision energy management and passenger safety, while maintaining or reducing vehicle weight, which in turn results in a better fuel economy [6–8]. Although the use of AHSS in the automotive industry is rapidly increasing, high strength low alloy (HSLA) steel is still predominately used in structural applications for manufacturing automotive parts. Some applications require higher elongations than those feasible with HSLA or superior strength compared to low carbon steel and other conventional heat-treated automotive steels [9]. In addition, due to the lower alloy content, HSLA also has better weldability compared to high alloy steel as well as provides excellent ductility with low strength. The research into resistance spot welding of HSLA steel with AHSS steel was published in [10, 11].

Hot-dip galvanized steel sheets are still preferred material for car body constructions. Two types of coatings are generally applied to steel sheets used in the automotive industry, namely galvanize and galvanneal coatings. Galvanize coatings contain essentially pure zinc with about 0.3 to 0.6 wt-% aluminium. A galvanneal coating is obtained by additional heating of the zinc-coated steel at 450–590°C immediately after the steel exits the molten zinc bath [12, 13].

Due to the diffusion of iron and alloying with zinc, the final coating contains around 90% zinc and 10% iron. Moreover, due to the alloying of zinc in the coating with diffused iron, there is no free zinc present in the galvanneal coating. HDGA coatings contain less aluminium than HDGI coatings, about 0.15 to 0.4 wt-%. Using of surface-treated steel sheets in automotive industry causes problems in the optimization of welding parameters. The pollution of welding electrode tips changes the contact resis-

***Corresponding Author: Ján Viňáš:** Technical University of Košice, Letná 9, 042 00 Košice, Slovakia; Email: jan.vinas@tuke.sk
Ľuboš Kaščák: Technical University of Košice, Letná 9, 042 00 Košice, Slovakia; Email: lubos.kascak@tuke.sk
Miroslav Greš: Technical University of Košice, Letná 9, 042 00 Košice, Slovakia; Email: miroslav.gres@tuke.sk

Table 1: Chemical composition of observed materials (in wt-%).

Material	C_{max}	Mn_{max}	Si_{max}	P_{max}
H260 LAD	0.1	0.6	0.5	0.025
H340 LAD	0.1	1.0	0.5	0.025
Material	S_{max}	Ti_{max}	Nb_{max}	Al_{min}
H260 LAD	0.025	0.15	0.09	0.015
H340 LAD	0.025	0.15	0.09	0.015

Table 2: Basic mechanical properties of observed materials.

Material	$Rp_{0.2}$ [MPa]	R_m [MPa]	A_{80} [%]
H260 LAD	260-330	350-430	26
H340 LAD	340-420	410-510	21

tances, which have a negative influence on welds' quality as well as welding tips lifetime [14]. The quality and mechanical behaviour of resistance spot welds significantly affect the durability and crashworthiness of vehicle [15]. Generally, spot weld failures occur in two modes: interfacial and pullout [13, 14]. The interfacial mode failure occurs through nugget, while the pullout failure mode occurs by complete (or partial) nugget withdrawal from one the joined sheet. The load-bearing capacity and energy absorption capability of those welds which fail under the overload interfacial mode are lower than those welds which fail under the overload pullout mode [15–17]. The welding parameters – current, time and pressing force have a significant influence on the quality of resistance spot welded joints. The effect of RSW welding time on mechanical properties of car body sheets was studied in [18]. However, because the weld nugget is invisible, the quality of welding in the welding process is not easy to judge. The traditional approach for evaluating weld's quality is by destructive testing. Some researchers have tried to use resistance spot welding surface image as an information source to evaluate the quality of resistance spot welding [19]. The core of the fractal theory is to start from a macro perspective, using related information of image in larger field of vision to process images. Fractal geometry provides people with the ideas and methods of irregular geometry. Fractal dimension can characterize some features of the image obtained in nature [20], which are effective parameters that can distinguish different image regions and textures roughness.

The research presents the results of the evaluation of welding current influence on the quality of spot welds of car body micro-alloyed steel sheets H260 LAD and H340 LAD.

2 Experimental methods

The hot-dip galvanized steel sheets H260 LAD EN 10292/2000 and H340 LAD EN 10292/2000 with the thickness of 1.0 mm were used for the experiments. The chemical composition and basic mechanical properties of these steel sheets are shown in Table 1 and Table 2.

The heat required for these resistance welding processes is produced by the resistance of the joined materials to an electric current. The amount of heat generated depends upon three factors; the amperage, resistance of the conductor and the duration of current [21]. These three factors affect the heat generated as expressed in the formula

$$Q = I^2 Rt \tag{1}$$

where Q is the heat generated (J), I is the current (A), R is the resistance of the work (Ω) and t is the duration of current (s).

According to Joule law (1), the most important parameter affecting the amount of heat obtained is welding current I. The welding current decreases with increasing resistance and induction in constant secondary voltage. The constant welding current affecting the weld joint is only maintained by constant resistance and induction. Inadequate heat energy cannot be achieved by bonding. However, excess welding current causes void and crack formations, partially spurt out of molten metal and so the tensile-shear strength of joint decreases [10, 14, 22].

The samples with dimensions of 40 × 92 mm and 32 mm lapping according DIN 50 124 standard were used for the experiments. The sample's surfaces were degreased in concentrated CH3COCH3 (acetone) before welding to eliminate the negative influence of impurities on the welding process and quality of spot welds.

Resistance spot welding of the samples was carried out on a pneumatic spot welding machine BPK 20, produced by VTS ELEKTRO Bratislava. The welding electrodes CuCr per ON 42 3039.71 standard were used in the experiments. The diameter of the working area of the electrode tips was d_e = ⌀5.0 mm. The parameters of resistance spot welding (welding current I, welding time t and pressing force of electrode *Fzv*) were determined in accordance with the recommendation of welding parameters by IIW - International Institute of Welding and based on previous research [5, 10]. All these parameters (Table 3) ensured the formation of fusion welded joints. The resistance spot welding cycle is shown in Fig. 1.

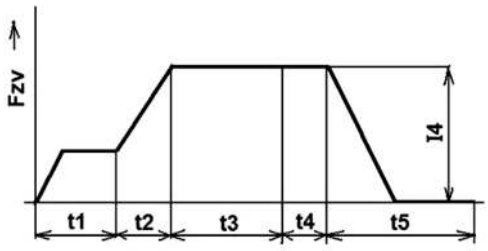

Figure 1: Welding cycle (Fzv – pressing force of electrodes, t – welding time, I – welding current).

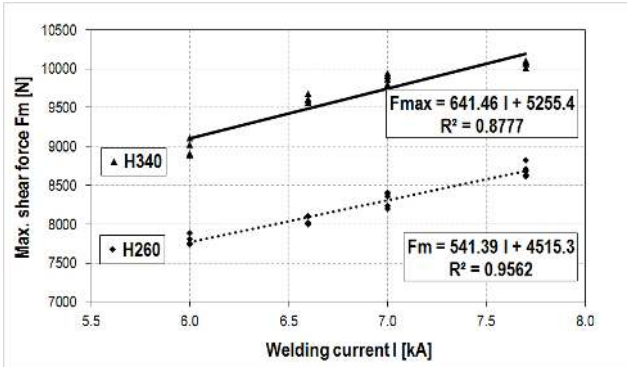

Figure 2: Dependency of load-bearing capacity of spot welds Fm on welding current I.

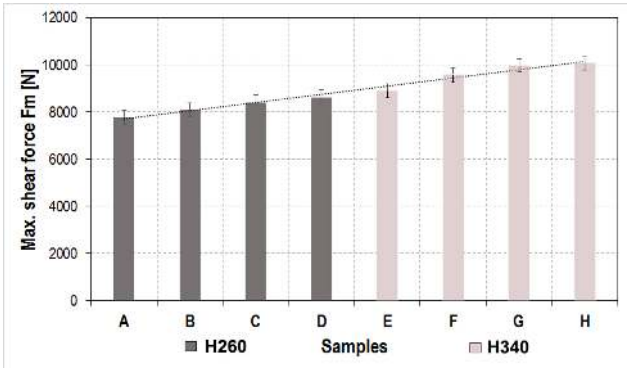

Figure 3: Average values of load-bearing capacities of welded joints.

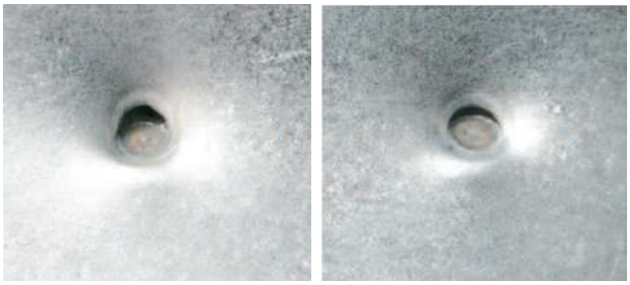

Figure 4: Failure of the spot welds after tensile test: a) H260 steel, b) H340 steel.

Table 3: Welding parameters for steel sheets (A, B, C, D – H220 LAD), (E, F,G, H – H340 LAD).

Welding parameters		Samples			
		A / E	B / F	C / G	D / H
Fzv	[kN]	2.6	2.6	2.6	2.6
t1	[per.]	10	10	10	10
t2	[per.]	9	9	9	9
t3	[per.]	12	12	12	12
t4	[per.]	8	8	8	8
t5	[per.]	12	12	12	12
I3	[kA]	4.0	4.6	5.0	5.7
I4	[kA]	6.0	6.6	7.0	7.6

The load-bearing capacities of the spot welded joints were evaluated according to standard DIN 50 124. This static tensile test was used for measuring the maximum force F_{max} until failure of the welds occurred. The test was conducted on the metal strength testing machine TIRAtest 2300 produced by VEB TIW Rauenstein, with the loading speed of 8 mm/min.

The quality of welded joints was evaluated by metallographic analysis on the light microscope Olympus TH 4-200. The scratch patterns for metallographic analysis were etched in 3% Nital solution.

3 Results and discussion

The dependency of load-bearing capacity of spot welds expressed as maximum shear force F_m on welding current I is shown in Fig. 2. Increasing of the welding current led to increasing of the maximum shear force in both type of materials. The values of load-bearing capacity of welded joints ranged from 7739 N to 8823 N for H260 LAD steel and from 8885 N to 10099 N for H340 LAD steel.

The average values of load-bearing capacity of resistance spot welded joints obtained from static tensile test are shown in Fig. 3.

Only the fusion welded joints occurred in all observed samples with typical failure during static tensile test – Fig. 4. The highest values of load-bearing capacity of H260 LAD steel sheets were measured on samples D, joined with the welding current of 7.6 kA. The load-bearing capacity of samples D increased by about 11% in comparison with samples A, joined with the welding current of 6.0 kA. The maximum values of load-bearing capacity of H340 LAD sheets were measured in samples H, joined with the maximum welding current of 7.6 kA as well. In comparison with samples E, that was welded with the lowest value of weld-

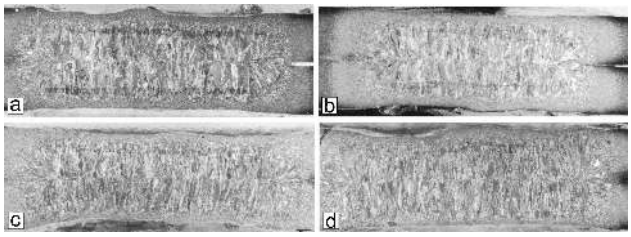

Figure 5: Macrostructures of the welds of H260 LAD steel: a) sample A (I=6.0kA), b) sample B (I=6.6kA), c) samples C (I=7.0kA) and d) sample D (I=7.6kA).

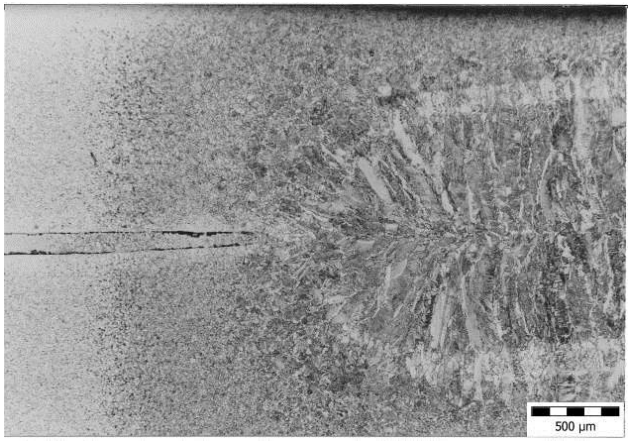

Figure 6: Microstructure of transition from the base metal to the weld nugget in sample A.

Figure 7: Microstructure of weld metal in the middle of weld nugget of sample B.

ing current of 6.0 kA, the load-bearing capacity increased by about 13%.

The results of the static tensile test of welded joints of H340 LAD sheets showed that an increase in the welding current from 7.0 kA to 7.6 kA resulted in an increase in the average maximum shear force of about 118 N. The results of the welded joints of H260 LAD sheets showed that the same increase of welding current led to increasing of the average maximum shear force of about 221 N.

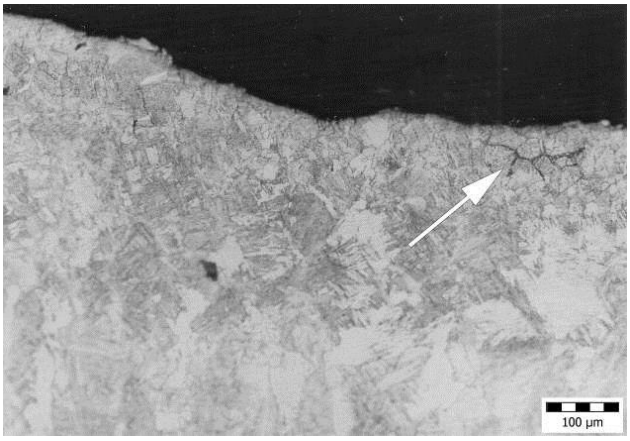

Figure 8: Cracks in the surface area of sample C.

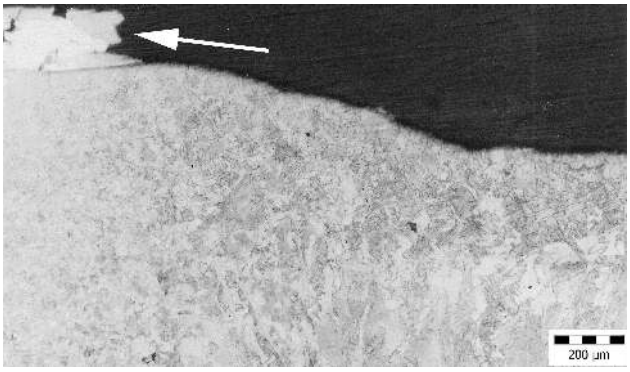

Figure 9: Microstructure of the heat affected zone of sample C with presence of brass.

Fig. 5 shows the macrostructures of welded joints of samples A, B, C and D. The fusion welded joints with a characteristic structure without any macroscopic defects occurred.

The dimensions of spot welds correspond to the used welding parameters and diameter of the welding electrode tips. Fig. 6 shows characteristic areas of a resistance spot weld – base metal, heat affected zone and weld nugget.

The dendritic microstructure of the weld nugget of sample B can be seen in Fig. 7.

Small cracks were observed in the microstructure of sample C, near the area of the weld nugget. The depth of the crack was approximately 50 µm and its length was about 90 µm, as can be seen in Fig. 8. The weld nugget dimensions of sample C are bigger than those in samples A and B. The width of the weld nugget exceeds the width of electrodes' contact area. The brass layer was observed near the contact area of the electrode and the weld surface was confirmed by EDX analysis (Fig. 9). This brass

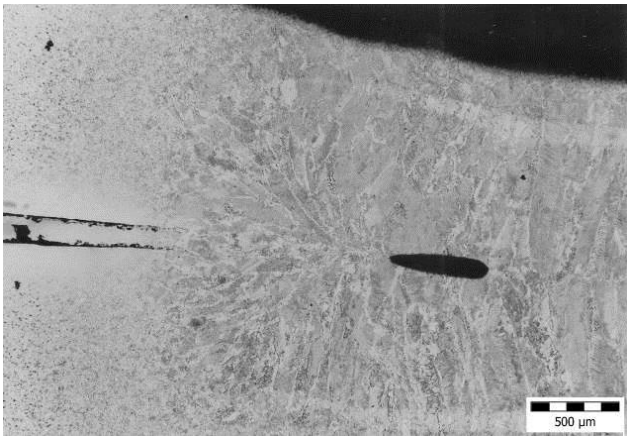

Figure 10: Microstructure of the weld with a cavity in the middle of nugget of sample D.

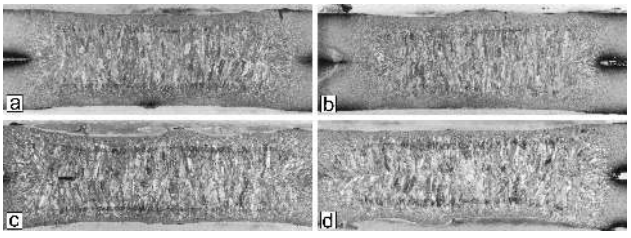

Figure 11: Macrostructures of the welds of H340 LAD steel: a) sample E (I=6.0kA, b) sample F (I=6.6kA, c) samples G (I=7.0kA) and d) sample H (I=7.6kA).

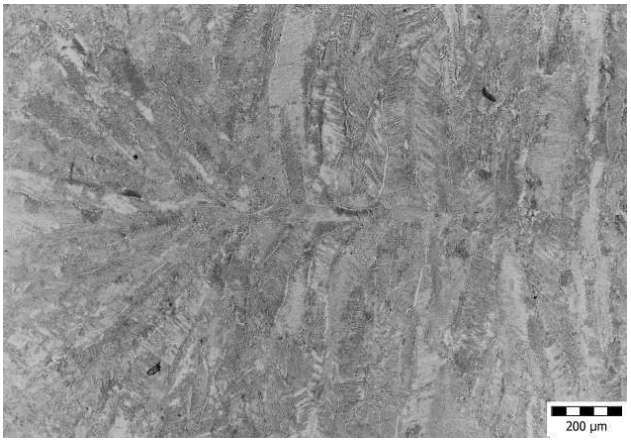

Figure 12: Microstructure of the weld nugget of sample E.

layer occurred on the surface of welding tips as well as on the zinc surface of welded sheets and has a negative effect on the contact resistance in the welding process. Because of a high welding temperature (906°C) and pressure, zinc evaporates from the welding area. On the other hand, if the temperature is lower (about 420°C), zinc melts and then adheres to welding tips. When thin brass layer is formed, it is forced out to the weld's perimeter.

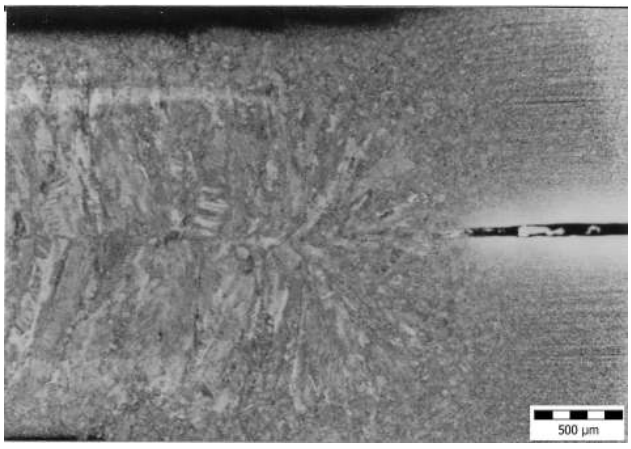

Figure 13: Weld nugget and heat affected zone of sample F.

The macrostructure of the weld made with welding current of 7.6 kA is shown in Fig. 5d. There is an elliptic cavity in the middle of the weld nugget (Fig. 10). No cracks or other failures occurred in the joint. The highest value of the welding current as well as the amount of generated heat led to the most significant grain coarsening and width growth of the heat affected zone in the weld metal in comparison with other samples.

The transition of the weld nugget into the base material of sample A are continual on both sides, as shown in Fig. 6. The weld nugget is symmetrical without any defects in the microstructure. There is a fine-grained structure of ferrite and unique occurrence of cluster pearlite around the weld nugget.

The weld macrostructure of sample E can be seen in Fig. 11a, with no macroscopic defects. Fig. 12 presents the weld metal structure in the middle of the weld nugget of sample E with hypoeutectoid ferrite and bainite.

The weld macrostructure of sample F with no macroscopic defects is shown in Fig. 11b. However, the microstructure analysis (Fig. 13) discovered a small crack with length of about 0.1 mm at the interface between the heat-affected zone and the weld nugget. The microstructures of the weld nugget and transition areas are like those of sample E.

The weld of sample G consists of cavity (Fig. 11c) and microcracks (Fig. 14), which is not acceptable from macroscopic and microscopic view.

The macrostructure of sample H is documented in Fig. 11d. There were no failures observed in the weld. The microstructure is relatively of high quality. The width of the weld nugget exceeds the width of electrodes' contact area.

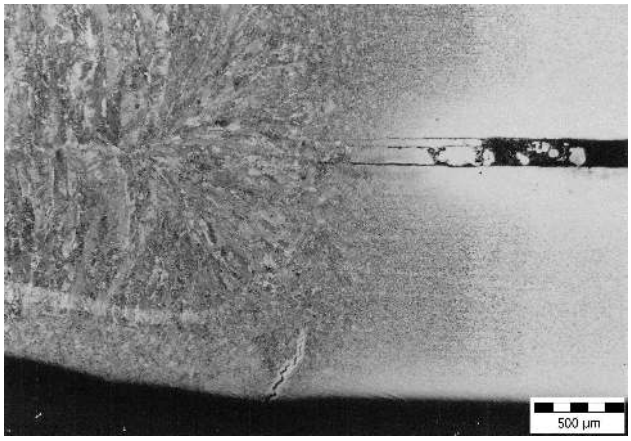

Figure 14: Cracks in heat affected zone of sample G.

4 Conclusions

The paper presents the results from the evaluation of the influence of the welding current on the quality of resistance spot welded joints of hot-dip galvanized micro-alloyed steel sheets. Based on the obtained results, it can be stated that:

- the increase in the welding current also increased the load-bearing capacity in both types of material,
- the lowest values of load-bearing capacity were measured in samples welded with welding current of 6.0 kA and the highest values were measured in samples welded with welding current of 7.6 kA,macro and microscopic analyses showed that spot welded joints with no defects were present on samples welded with the welding current of 6.0 kA for H260 sheets and 6.6 kA for H340 sheets.

Acknowledgement: The research was supported by the Slovak Research and Development Agency under contract APVV-0273-12 "Supporting innovations of autobody components from the steel sheet blanks oriented to the safety, the ecology and the car weight reduction".

References

[1] Zhang H., Wang F, Xi T., Zhao J., Wang L., Gao W., A novel quality evaluation method for resistance spot welding based on the electrode displacement signal and the Chernoff faces technique, Mech. Syst. Signal Pr., 2015, 62–63, 431–443

[2] Tan J. C., Westgate S. A., Clyne T. W., Resistance welding of thin stainless steel sandwich sheets with fibrous metallic cores: experimental and numerical studies, Sci. Technol. Adv. Mater., 2007, 12, 490–504

[3] Moshayedi H., Sattari-Far I., Resistance spot welding and the effects of welding time and current on residual stresses, J. Mater. Process. Technol., 2014, 214, 2545–2552

[4] Wei P.S., Wu T.H., Electrode geometry effects on microstructure determined by heat transfer and solidification rate during resistance spot welding, Int. J. Heat Mass Tran., 2014, 79, 408–416

[5] Spišák E., Kaščák Ľ., Viňáš J., Research into properties of joints of combined materials made by resistance spot welding, Chem. Listy, 2011, 16, 488–490

[6] Pouranvari M., Susceptibility to interfacial failure mode in similar and dissimilar resistance spot welds of DP600 dual phase steel and low carbon steel during cross-tension and tensile-shear loading conditions, Mater. Sci. Eng., 2012, A 546, 129–138

[7] Wan X., Wang Y., Zhang P., Modelling the effect of welding current on resistance spot welding of DP600 steel, J. Mater. Process. Tech., 2014, 214, 2723–2729

[8] Wang J., Wang H.P., Lu F., Carlson B.E., Sigler D.R., Analysis of Al-steel resistance spot welding process by developing a fully coupled multi-physics simulation model, Int. J. Heat Mass Tran., 2015, 89, 1061–1072

[9] Saha D.C., Westerbaan D., Nayak S.S., Biro E., Gerlich A.P., Zhou Y., Microstructure-properties correlation in fiber laser welding of dual-phase and HSLA steels, Mater. Sci. Eng.: A, 2014, 607, 23, 445–453

[10] Kaščák Ľ., Mucha J., Slota J., Spišák E., Application of modern joining methods in car production, 1st ed., Oficyna Wydawnicza Politechniki Rzeszowskiej, Rzeszów, 2013

[11] Kaščák Ľ., Spišák E., Gajdoš I., Joining the combination of AHSS steel and HSLA steel by resistance spot welding, Acta Mech. Autom., 2013, 7, 75–78

[12] Zhigang H., Yuanxun W., Chunzhi Li, Chuanyao C., A multi-coupled finite element analysis of resistance spot welding process, Acta Mech. Solida Sin., 2006, 19, 86–94

[13] Pouranvari M., Analysis of Fracture Mode of Galvanized Low Carbon Steel Resistance Spot Welds, International Journal of Multidisciplinary Sciences and Engineering, 2011, 2, 36–40.

[14] Zhang H., Senkara J., Resistance welding: Fundamentals and Applications, 2nd ed., Taylor & Francis, New York, 2006

[15] Donders S., Brughmans M., Hermans L., Liefooghe C., Van der Auweraer H., Desmet W., The robustness of dynamic vehicle performance to spot weld failures, Finite Elem. Anal. Des., 2006, 42, 670–682

[16] Chao Y.J., Failure of Spot Welds: Interfacial versus Pullout, Sci. Technol. Weld. Joi., 2003, 8, 133–137

[17] Pouranvari M., Asgari H.R., Mosavizadeh S.M., Marashi P.H., Goodarzi M., Effect of weld nugget size on overload failure mode of resistance spot welds, Sci. Technol. Weld. Joi., 2007, 12, 217–225

[18] Aslanlar S., Ogur A., Ozsarac U., Ilhan E., Welding time effect on mechanical properties of automotive sheets in electrical resistance spot welding, Mater. Des., 2008, 29, 1427-1431

[19] Zhanfeng H., Pei W., Jing X., Jingyu H., Application of fractal theory in examination of resistance spot welding quality, In: International Conference on Advanced Technology of Design and Manufacture (23-25 November 2010, Beijing, China), Institution of Engineering and Technology, 2010, 422–424

[20] Hu Y., He J.H., On fractal space-time and fractional calculus, Therm. Sci., 2016, 20, 773–777

[21] Aslanlar S., Ogur A., Ozsarac U., Ilhan E., Demir Z., Effect of welding current on mechanical properties of galvanized chromided steel sheets in electrical resistance spot welding, Mater. Des., 2007, 28, 2–7

[22] Pouranvari M., Effect of Welding Current on the Mechanical Response of Resistance Spot Welds of Unequal Thickness Steel Sheets in Tensile-Shear Loading Condition, Ma-ter. Sci. Eng., 2011, 2, 63–67